JGR Earth Surface

RESEARCH ARTICLE
10.1029/2020JF005597

Special Section:
The Three Major Hurricanes of 2017: Harvey, Irma and Maria

Hurricane Deposits on Carbonate Platforms: A Case Study of Hurricane Irma Deposits on Little Ambergris Cay, Turks and Caicos Islands

Sarah Jamison-Todd[1], Nathan Stein[2], Irina Overeem[1], Arslaan Khalid[3], and Elizabeth J. Trower[1]

[1]Department of Geological Sciences, University of Colorado Boulder, Boulder, CO, USA, [2]Division of Geological and Planetary Sciences, California Institute of Technology, Pasadena, CA, USA, [3]Department of Civil, Environmental and Infrastructure Engineering, George Mason University, Fairfax, VA, USA

Key Points:
- Hurricane deposits on a carbonate platform have characteristics unique to this geological setting
- High storm surges and flow velocities cause sediment bypass that leaves behind small, unstructured deposits
- The identification of massive carbonate beds adjacent to erosional features may aid in identifying storm events in the rock record

Supporting Information:
- Supporting Information S1

Correspondence to:
S. Jamison-Todd,
saja4038@colorado.edu

Citation:
Jamison-Todd, S., Stein, N., Overeem, I., Khalid, A., & Trower, E. J. (2020). Hurricane deposits on carbonate platforms: A case study of Hurricane Irma deposits on Little Ambergris Cay, Turks and Caicos Islands. *Journal of Geophysical Research: Earth Surface*, *124*, e2020JF005597. https://doi.org/10.1029/2020JF005597

Received 29 FEB 2020
Accepted 25 JUN 2020
Accepted article online 26 JUN 2020

Abstract The study of modern hurricane deposits is useful in both identifying ancient hurricane deposits in the rock record and predicting patterns of deposition and erosion produced by future storm events. Hurricane deposits on carbonate platforms have been studied less frequently than have been those along continental coasts. Here we present observations of the characteristics of deposition and scour caused by Hurricane Irma on Little Ambergris Cay, a small uninhabited island located near the southeastern edge of the Caicos platform in the Turks and Caicos Islands. Hurricane Irma passed directly over Little Ambergris Cay on 7 September 2017 as a Category 5 hurricane. We described and sampled multiple types of hurricane deposits and determined that the washover fans were the best sedimentological records for hurricane conditions, as they were subject to very little reworking over time. We compared different model predictions of storm tide and wave height with eyewitness reports and distributions of scour. Examining the washover fans allowed for the construction of a conceptual model for hurricane deposits formed in a high-energy storm event on a carbonate platform. Characteristics of the washover fans were their small size, the lack of sedimentary structures, and very well sorted sediment. The size and distribution of carbonate boulders eroded and transported by the storm are consistent with depth-averaged flow velocities in the range of 1.5–5.3 m/s. The strength of the storm and the low-lying topography, distinct features of a carbonate platform setting, contributed to high levels of sediment bypass and high flow velocities, resulting in small, unstructured deposits.

1. Introduction

Washover fans are the product of near-instantaneous depositional events (Morton & Sallenger, 2003) that represent the flow conditions during major storm events that produce surges, tsunamis, or high waves and are unique depositional records that can be used to reconstruct those conditions. The deposits typically form when a landward storm surge overreaches or breaches the height of the local topography (Lazarus, 2016). Fans are formed landward of the shore edge and stretch in the direction of flow and sediment transport (Hudock et al., 2014). They are often lobate and associated with a "throat," or shallow channel or drainage feature (Hudock et al., 2014; Lazarus, 2016). Peak deposition commonly occurs as the flow velocities associated with the storm ebb. Washover fans are a common depositional feature of areas exposed to extreme weather (Morton & Sallenger, 2003), and numerous studies have reported expected dimensions and sedimentary trends involving grain size and sedimentary structures. The majority of studies previously conducted on hurricane deposits examined washover fans on barrier islands or continental coastal environments, where sediment bodies of this type are most commonly found after a storm event (Deery & Howard, 1977; Hudock et al., 2014; Leatherman & Williams, 1977; Leatherman & Williams, 1983; Morton & Sallenger, 2003; Spiske & Jaffe, 2009; Schwartz, 1982; Sedgwick & Davis Jr., 2003; Soria et al., 2018; Wanless et al., 1988; Wang & Horowitz, 2007). There are consistent observed sediment trends between the results of most of these studies.

Commonly reported characteristics of washover fan deposits in continental coastal environments include the following: graded or inversely graded bedding (Leatherman & Williams, 1983; Schwartz, 1982; Sedgwick & Davis, 2003; Spiske & Jaffe, 2009; Soria et al., 2018; Wanless et al., 1988; Wang & Horowitz,

2007), tabular landward-dipping beds (Deery & Howard, 1977; Hudock et al., 2014; Schwartz, 1982; Sedgwick & Davis, 2003, Shaw et al., 2015; Wang & Horwitz, 2007), and lateral as well as vertical grading (Leatherman & Williams, 1977; Schwartz, 1982). By far the most commonly observed feature is graded bedding followed by the tabular landward-dipping beds that are often observed with large, nonephemeral fans that are formed by multiple storm surge events. Additionally, large storm events and associated seaward storm surges have been known to cause high levels of sediment bypass and net sediment loss on barrier islands, with regions of erosion and deposition often proximal to one another (Goff et al., 2019; Sallenger, 2000; Sherwood et al., 2014).

Modern carbonate platforms in the Atlantic hurricane belt (subject to counterclockwise storm circulation) are frequently traversed by hurricanes but are less often studied than are other coastal areas. Conditions producing sedimentation and forming bathymetric profiles on and adjacent to carbonate platforms can vary from other depositional environments (Williams et al., 2011; Wilson, 1974). The bathymetry is shallow on top of the Caicos carbonate platform but forms an abrupt transition from deep-marine to shallow-marine depositional environments at the edge of the platform (Harris & Ellis, 2008). This bathymetry contrasts with that of continental shelf margins, which, while often composed of both carbonate and clastic material, tend to have more gradual slopes moving inland as well as more complex bottom structures associated with complex continental tectonics (Bergantino, 1971; Bryant et al., 1968). Carbonate platform deposits are common in the rock record, and using a modern analogy to understand their associated hurricane deposits in greater detail can potentially help to identify their sedimentary signature in ancient carbonate settings (Read, 1982; Pomar, 2001).

The signature of storm deposits on a low-elevation carbonate island has been the subject of few studies (Boss & Neumann, 1993; Mattheus & Fowler, 2015; Reeder & Rankey, 2009; Wanless et al., 1988; Wilson et al., 2018). Those studies that have been conducted on the geomorphological impact of major hurricanes in carbonate platform environments have found that there is minimal observable deposition related to these events and no notable deposits analogous to washover fans (Boss & Neumann, 1993; Reeder & Rankey, 2009). Analogously, indundation of barrier islands and atolls subjected to major storm events is often associated with lower levels of deposition than on higher-elevation islands that block storm surges and trap sediment (Lindemer et al., 2010; Sallenger, 2000; Sherwood et al., 2014).

To better understand why the sedimentation processes associated with a major storm event on a carbonate platform result in apparently minimal deposition, we characterized recent deposits from Hurricane Irma (September 2017) on Little Ambergris Cay (LAC), Turks and Caicos Islands. We characterized sediment properties such as grain size, roundness, and sorting and addressed dimensions of deposits and sediment volume. Areas of erosion and adjacent sediment composition were examined to make interpretations about sediment sourcing and flow conditions. We used a variety of estimates and numerical modeling to estimate storm surge and wave heights. Flow velocities were calculated using measurements of dimensions of large clasts to reconstruct storm conditions and potential depositional and erosional processes occurring during the hurricane. We applied these observations to develop a conceptual framework for identifying and interpreting washover fan deposits in ancient carbonate platform successions.

2. Methodology

2.1. Study Site

This study focuses on LAC, an ~6-km-long, maximally ~1.6-km-wide uninhabited island on the Caicos platform in the Turks and Caicos Islands. The Caicos platform is a shallow-marine carbonate shelf with a collection of low-level islands of Pleistocene origin composed of lithified carbonate rock (Kerans et al., 2019) and unconsolidated oolitic, skeletal, and peloidal sand (Dravis & Wanless, 2008, 2017). The sediment on LAC is almost exclusively composed of ooids, with a minor component of skeletal sand (Trower et al., 2018). The island is dominated biologically by microbial mats, with some bays and interior zones of mangroves, and brushy vegetation along the beach ridges. Unlike other islands on the Caicos platform, the lithified areas of LAC are exclusively Holocene in age (Orzechowski et al., 2016).

Hurricane Irma passed directly over the island on 7–8 September 2017 as a Category 5 hurricane with 1-min sustained winds of 170 mph (274 kph), making LAC an ideal location to study the deposits formed during the

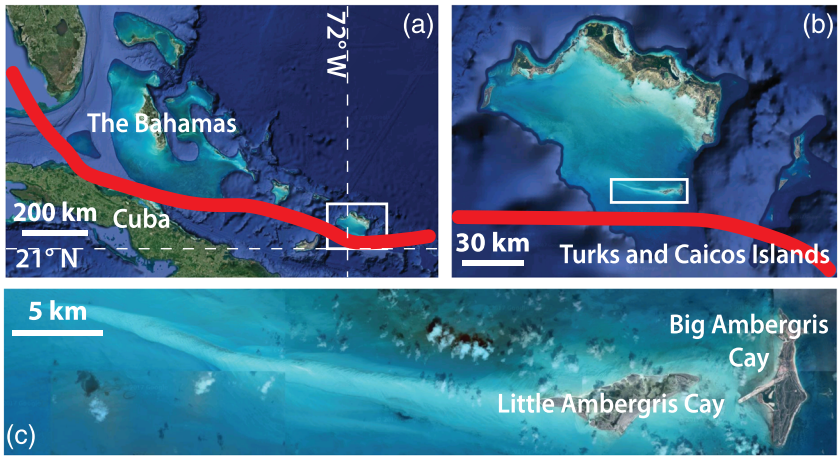

Figure 1. (a) Satellite location map of the Turks and Caicos Islands with the storm track of Hurricane Irma superimposed. (b) Inset showing the area indicated by the white box in (a); (c) inset showing the area indicated by the white box in (b). Storm track data from 2017 NOAA report; satellite images from Google and DigitalGlobe. Figure modified after Figure 2 in Trower et al. (2018).

hurricane (Figure 1). LAC was located directly in the path of the hurricane, with the eye of Hurricane Irma traversing the island roughly east to west during the passage of the storm. Counterclockwise circulation as the storm passed over the island subjected LAC first to a southward storm surge associated with the leading arm of the storm and then to a northward storm surge associated with the trailing arm of the hurricane. Pressure was observed to average ~920 mbar on 7 September 2017 (Cangialosi et al., 2017).

We used a large-domain hydrodynamics model, the Advanced Circulation model (ADCIRC) (Luettich et al., 1992) tightly coupled to the Simulating WAves Nearshore (SWAN) model (Booij et al., 1999; Dietrich et al., 2011), to estimate water level heights, storm surge, and significant wave height in the nearshore zone of LAC (Egbert & Erofeeva, 2002; Garzon et al., 2018; Li et al., 2013; Sahoo et al., 2019; Westerink et al., 2008). The model domain was set up as an unstructured grid (Roberts et al., 2019), allowing for ingestion of detailed bathymetry of the shallow carbonate platform (Harris & Ellis, 2008) and the shoreline of LAC (supporting information Figures S1 and S2) (Tozer et al., 2019; Wessel & Smith, 1996). Hindcasted parameters (storm track, radius of maximum winds, minimum central pressure, maximum sustained winds, etc.) pertaining to Hurricane Irma were extracted from the National Hurricane Center's HURicane DATabase (HURDAT2). These parameters were then used to calculate the wind and pressure forcing at each vertex of the numerical mesh. The resulting wind stresses were used by the SWAN model to capture the increase in water levels as a result of wave energy nearshore. ADCIRC-SWAN predictions were tracked over the duration of Hurricane Irma at seven "observation stations" surrounding the island. The modeled water level crests at 3.2 m on the south side of LAC, whereas the water level on the northern side of the island peaked at a more modest 2 m (supporting information Figure S4). Significant wave heights were hindcasted to be around 1.2 m on the south side and ~1 m on the north side of LAC (Figures 2 and S5). The modeled water level exceeded local berm height for >3 hr on 8 September over the duration of the passing of Hurricane Irma. Our model treated the island as a closed boundary and did not simulate flow across the lithified berm, vegetated sand berms, or mangroves. However, we do infer that interior flow was S-N for >3 hr based on higher water levels simulated on the southside of the island. We provide details on the model setup, validation, and results in the supporting information.

Modeled water level heights are corroborated by observations of scour height in a lithified channel on LAC, which achieved a depth at the peak of the hurricane of about 3.5 m and eyewitness observations from the long-time island manager (P. Mahoney, personal communication, March 26, 2018). The highest elevation point on LAC is ~4 m, and beach ridges are ≤1.7 m high (supporting information Figure S8); the submersion of the island was therefore nearly complete during the 3-hr peak of the storm surge.

Our observations were compared with those of previous studies (Deery & Howard, 1977; Hudock et al., 2014; Lazarus, 2016; Leatherman & Williams, 1977, 1983; Morton & Sallenger, 2003; Schwartz, 1982; Sedgwick &

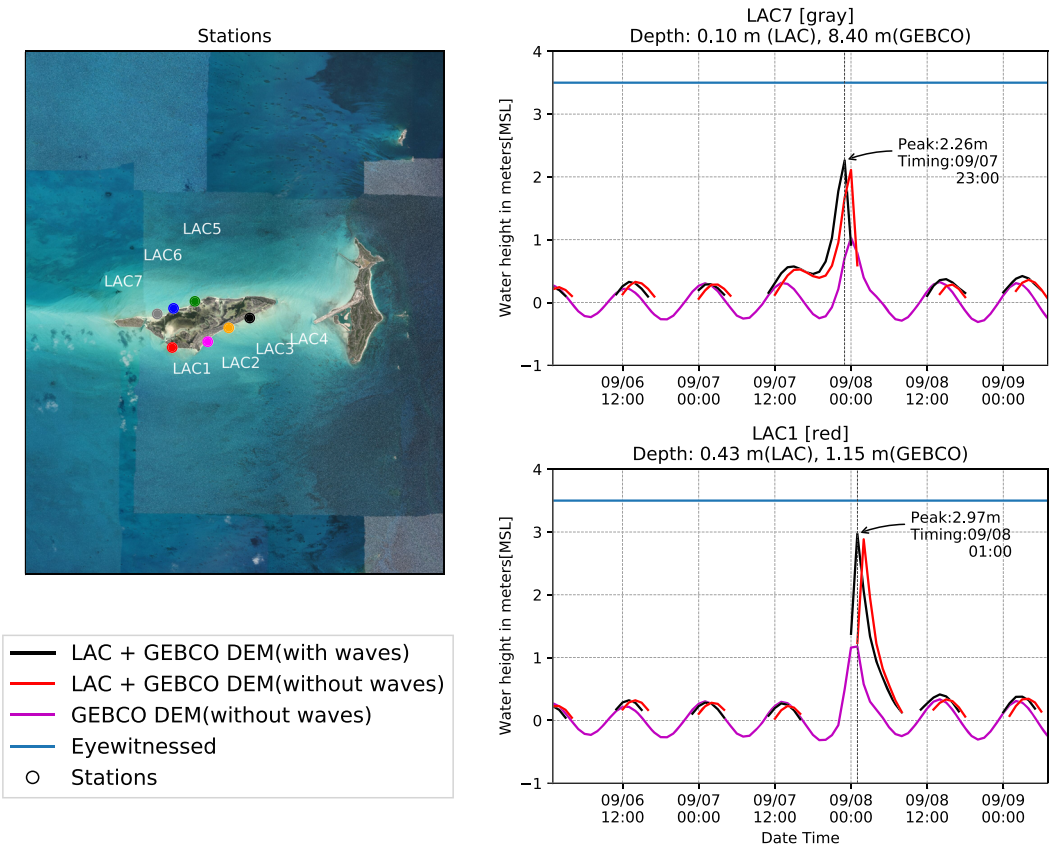

Figure 2. Time series of simulated storm surges in meters above mean sea level around Little Ambergris Cay during Hurricane Irma (September 2017). Representative stations at the north and south side of the island are shown here.

Davis, 2003; Soria et al., 2018; Spiske & Jaffe, 2009; Wang & Horowitz, 2007; Wanless et al., 1988) dealing with similar sediments (sands in beach settings) in similar environments (coasts along continental margins and barrier islands). Barrier islands share some characteristics with the small cays in the Turks and Caicos Islands, as they are commonly partially lithified, of low elevation, and inundated by major storm events (Sherwood et al., 2014; Wesselman et al., 2019). These previous studies served as a guideline for expected dimensions and sediment trends to contrast with what we observed on LAC.

2.2. Sample Collection and Field Observations

Sediment samples from the hurricane deposits were collected in March and July of 2018 and June of 2019 (6, 10, and 21 months after Hurricane Irma, respectively). Samples were collected from multiple deposits at several depths, in order to observe any lateral or vertical grading. Changes in sediment sorting were also examined to determine if there were fluctuations in flow energy over the course of the storm event.

The sediment bodies sampled included washover fans in the interior of the island, lobes at the mouths of tidal channels on the northern side of the island, beach ridges adjacent to the washover fans, and the supratidal beach and foreshore on the southern side of the island (Figure 3). Fifty-seven sediment samples were collected in March 2018, 33 in July 2018, and 11 in June 2019; sediment samples were collected in 15-ml centrifuge tubes. The channel lobes were originally sampled in March 2018 and resampled in July 2018 to determine the role of current reworking. In July 2018 an ~1-m-long sediment core was collected via vibracoring in one of the washover fans in order to compare the Hurricane Irma deposits with underlying deposits. Samples were collected in 15-ml centrifuge tubes every ~4 cm along the length of the core. All samples were rinsed, dried, and analyzed using a Retsch Camsizer P4 at the University of Colorado Boulder to document grain size, roundness, and sorting.

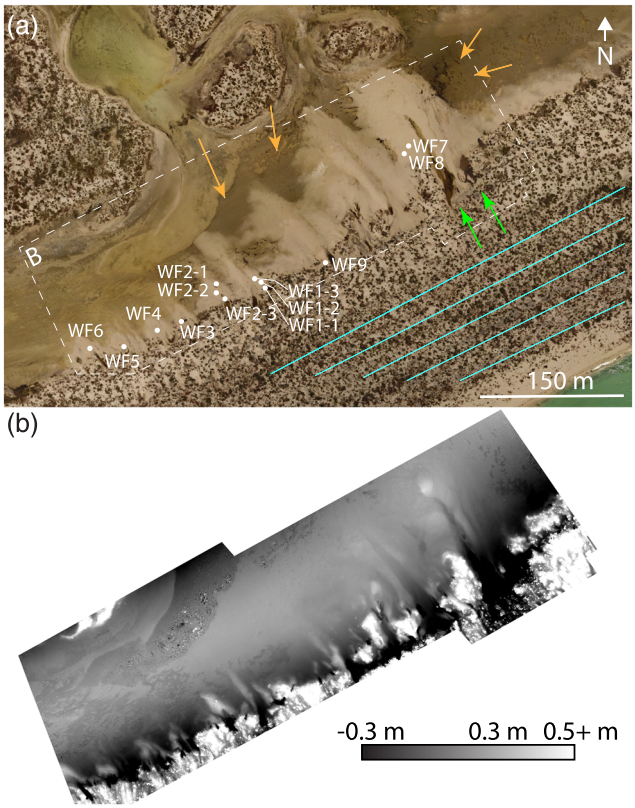

Figure 3. (a) Washover fan sample locations and (b) the digital elevation model of the washover fan area. In (a), turquoise lines indicate the beach ridge area, and green arrows indicate two of the larger scour pits. Scour pits are present adjacent to each of the washover fans on either side. Major microbial mat areas adjacent to the washover fans are indicated by orange arrows.

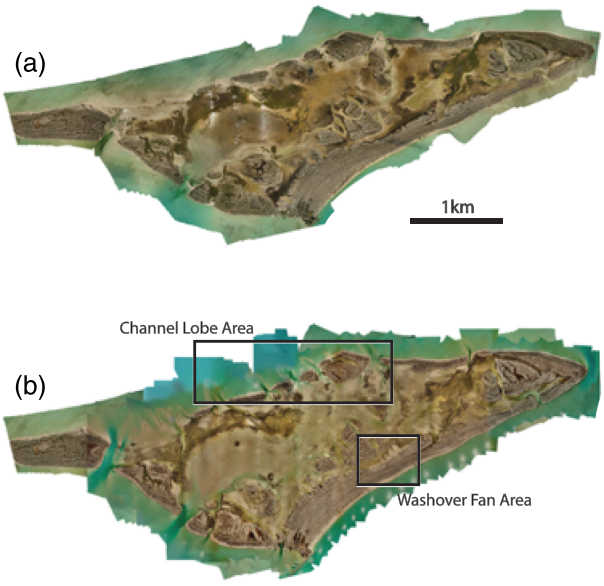

Figure 4. Drone orthomosaic maps of Little Ambergris Cay in 2017, before (a) and after (b) Hurricane Irma.

The washover fans were surveyed with a DJI Phantom 4 Pro drone with a 20-megapixel color camera in September 2017, March 2018, July 2018, and June 2019 to observe their modification. The surveys were conducted from 150-m altitude during each field period, yielding spatial resolutions of ~5.1 cm, and additionally from 30-m altitude in March 2018, July 2018, and June 2019, yielding spatial resolutions of ~7 mm (Figure 4).

Photogrammetric digital elevation models were generated from the low-altitude survey data at ~1.5-mm vertical resolution and ~7-mm lateral resolution using Agisoft Photoscan. The digital elevation models were used to examine how the topography of beach ridges on the island may have affected patterns of sediment deposition during the storm event. In addition to the high-resolution topographic data, a previously compiled facies map was used to note where differences in the types of microbial mat growth affected the size or sediment trends of the washover fans (Stein et al., 2016).

Tidal channel current velocities were measured with Lowell Instruments TCM-1 and TCM-4 tilt current meters, anchored with cinder blocks. Tidal variations in water depth on the island interior were measured with HOBO U20L water depth loggers. Data from HOBO loggers was corrected with local barometric data collected with an additional HOBO U20 logger deployed above water on LAC.

Dimensions of small boulders transported into the interior of the island during the storm were measured in order to calculate flow velocities into the island interior at the height of the hurricane. These clasts are tabular and have an average short axis dimension of 14.5 cm, within the range of a cobble grain size, but have an average intermediate axis dimension of 29 cm, exceeding the minimum for boulders, and are hereafter referred to as boulders. Calculated flow velocities were compared to those that would be required for transport of oolitic sand in bedload, suspended load, and washload, to identify the transport regime of sand during peak hurricane intensity. Ooid sand transport regimes were calculated using the Rouse number P, a dimensionless number that describes different modes of transport:

$$P = \frac{w_s}{\kappa u_*}, \tag{1}$$

where w_s is settling velocity (m/s), $\kappa = 0.41$ is von Karman's constant, and u_* is the bed shear velocity (m/s). The Rouse number $P = 7.5$ corresponds to the threshold for motion, $P = 2.5$ to bedload transport, $P = 1.2$ to 50% of sediment suspended, and $P = 0.8$ to sediment in washload. We used Camsizer measurements of median grain size (D_{50}) of washover fan sediment to calculate w_s, following Dietrich (1982):

$$w_s = (RgvW_*)^{1/3}, \tag{2}$$

where v is kinematic fluid viscosity and W_* is dimensionless settling velocity, calculated as

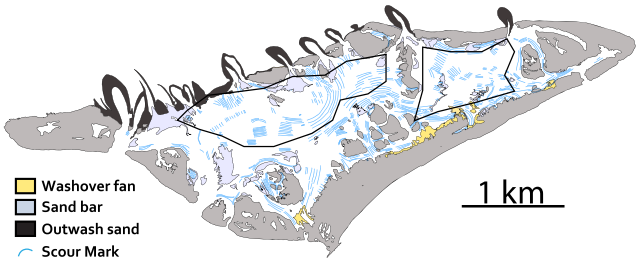

Figure 5. Hurricane deposit facies and flow lines in the interior lagoon during the storm, inferred from scour marks. Two major mangrove zones are outlined in black.

$$W_* = R_3 10^{(R_1+R_2)}. \tag{3}$$

R_1, R_2, and R_3 are empirically fitted equations that account for particle size, shape, and density, respectively:

$$R_1 = -3.76715 + 1.92944\log D_* - 0.09815(\log D_*)^2 - 0.00575(\log D_*)^3 + 0.00056(\log D_*)^4, \tag{4}$$

$$R_2 = \left(\log\left(1 - \frac{1-\mathrm{CSF}}{0.85}\right)\right) - (1-\mathrm{CSF})^{2.3}\tanh(\log D_* - 4.6) + 0.3(0.5-\mathrm{CSF})(1-\mathrm{CSF})^2(\log D_* - 4.6), \tag{5}$$

$$R_3 = \left[0.65 - \left(\frac{\mathrm{CSF}}{2.83}\tanh(\log D_* - 4.6)\right)\right]^{\left(1+\frac{3.5-\mathrm{PS}}{2.5}\right)}, \tag{6}$$

where $D_* = \frac{RgD^3}{\nu^2}$ is dimensionless particle size, CSF is the Corey shape factor (we assume the particles are spherical and use CSF = 1), and PS is the Powers roundness (assuming a spherical particle, we set PS = 6). We then solved for u_* at each Rouse threshold by rearranging Equation 1. Finally, we used the law of the wall equations to solve for depth-averaged flow velocity for each u_*:

$$u = \frac{u_*}{\kappa}\ln\left(\frac{z}{z_0}\right) \tag{7}$$

yields flow velocity as a function of depth, where z is the height above the bed and $z_0 = \frac{D_{50}}{10}$ is the bed roughness. Integrating this equation and dividing by the depth of flow, H, yield depth-averaged flow velocities ($<u>$) for the oolitic sand:

$$<u> = \frac{1}{H}\int_0^H \frac{u_*}{\kappa}\ln\left(\frac{z}{z_0}\right)dz, \tag{8}$$

where all other variables are as previously defined and H is the flow depth of 3.5 m. Flow velocities were calculated for a variety of depths to determine how storm surge depth controls transport.

Average boulder intermediate axis length and short axis length were 29 and 14.5 cm, respectively (see supporting information Table S2). Flow velocities required to transport clasts with these dimensions were calculated using the following equations from Nandasena et al. (2011) and Soria et al. (2018):

$$\text{Sliding: } u^2 \geq \frac{2\left(\frac{\rho_s}{\rho_w} - 1\right)gc\,(\mu_s\cos\theta + \sin\theta)}{C_d\left(\frac{c}{b}\right) + \mu_s C_l}, \tag{9}$$

$$\text{Rolling: } u^2 \geq \frac{2\left(\frac{\rho_s}{\rho_w} - 1\right)gc\left(\cos\theta + \left(\frac{c}{b}\right)\sin\theta\right)}{C_d\left(\frac{c^2}{b^2}\right) + C_l}, \tag{10}$$

$$\text{Lifting: } u^2 \geq \frac{2\left(\frac{\rho_s}{\rho_w} - 1\right) gc \cos\theta}{C_l}, \tag{11}$$

where ρ_s is the boulder density (2.85 g/cm^3), ρ_w is the density of seawater (1.025 g/cm^3), g is the acceleration due to gravity (9.81 m/s^2), c is the length of the shortest axis of the boulder, b is the length of the intermediate axis of the boulder, μ_s is the coefficient of static friction (0.5), θ is the angle of the bedslope (0°), C_d is the coefficient of drag (1.95), and C_l is the coefficient of lift (0.178) following Nandasena et al. (2011) and Soria et al. (2018). Following Nandasena et al. (2011), boulders are considered to be rectangular prisms, and the forces acting on the clasts are only drag, lift, inertia, and gravity. Flow velocities required to transport the oolitic sand grains and boulders were then compared. To constrain the flow velocities required to transport the boulders, we then used equations from Terry et al. (2013) and Nott (2003) to calculate upper and lower flow velocity thresholds for these estimates. High tides on LAC are at least 0.5 m deep (supporting information Figure S6), sufficient to submerge all of the measured clasts, so we can assume that with the addition of the storm surge the boulders were submerged above this minimum depth while in transport. All of the equations for boulders assume that flow depth is sufficient for transport. The sand transport calculations were determined for flow depths ranging from 0.5 to 4.5 m, bracketing the minimum surge level of 0.5 m (high tide) and the maximum calculated surge of 4.1 m to determine the role flow depth plays in the results of the calculations.

We recorded the dimensions of eight erosional scour pits adjacent to the washover fans and estimated their volume based on an approximation of a triangular trough (length × width × 0.5 (depth) = volume), in order to determine how much sediment was displaced by erosion during the storm event (supporting information Table S6). Similarly, we estimated washover fan volume by using fan dimensions to approximate a wedge.

Elemental composition analysis of washover fan ooids and beach ridge ooids was conducted using energy dispersive spectroscopy with a Hitachi SU 3500 scanning electron microscope with an accelerating voltage of 10 kV and a working distance of 10 mm, housed in the Colorado Shared Instrumentation in Nanofabrication and Characterization at the University of Colorado, Boulder, to determine the origin of the observed pink-tan color on these ooids. Ooids were mounted with carbon tape on aluminum stubs and coated with Pd prior to analysis.

3. Results

3.1. Descriptions of Island Characteristics and Hurricane Deposit Types

The low-elevation topography of LAC consists of beach ridges defining the edges of the island and a tidal lagoon in the interior of the island that is shallowly submerged and subject to gentle reworking by tides as water flows in and out of the lagoon (Figure 3). Vegetation on LAC consists of shrubs, bushes, and grasses between 30 and 200 m from the shore and beach. Closest to the beach, deeply rooted tussocks of sea oats (*Uniola paniculata*) occur. Beach ridge shrubs include sea grape trees (*Coccoloba uvifera*) of 0.8–1.2 m in height and 0.6- to 1.0-m-high manchineel trees (*Hippomane mancinella*). The remainder of the vegetation on LAC consists of dense mangrove patches, of both red and black mangroves (*Rhizopora mangle* and *Avicennia germinans*, respectively), covering 0.66 km^2 of the island's total 6.1-km^2 area. Early-lithified sand is exposed over 2.53 km^2.

The deposits formed during the storm consist of washover fans on the southern side of the island interior, channel lobes extending offshore on the northern side of the island, and lag deposits composed of either tabular intraclasts composed of lithified Holocene sediment or well-rounded microbial mat intraclasts (Figures 3b and 4). The locations and orientations of these depositional and erosional features are consistent with formation during the northward directed storm surge of the trailing arm of the storm. Scour pits are located south (i.e., upcurrent) of the washover fans, potentially reoccupying older scour features from previous hurricanes. Other erosional features consist of up to 3 m of vertical scour depth, straightening of tidal channels, and scoured sections of microbial mats. Some of these eroded microbial mats were subsequently deposited in microbial mat intraclast lag deposits (Figure 6). The washover fans and channel lobes formed during the hurricane are composed of oolitic sand. Any sand bodies formed during the passage of the leading arm of the storm would likely have been subsequently remobilized and erased by the passage of the trailing

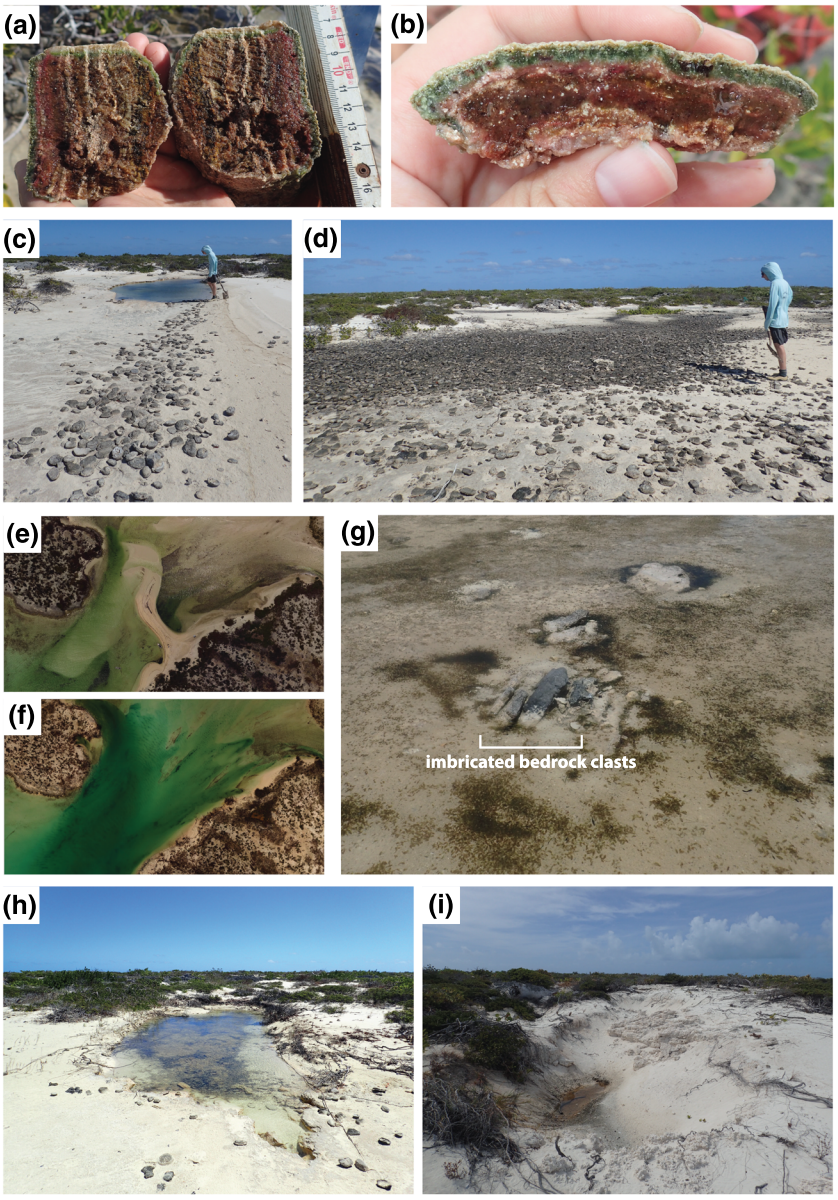

Figure 6. Images of erosional sedimentary features of Hurricane Irma on LAC. Cross sections of microbial mat intraclasts illustrating rounded edges due to erosion and varying morphologies—(a) equant and (b) tabular. Lag deposits of microbial mat intraclasts, which can range from (c) relatively small spatial extent and intraclast density to (d) larger spatial extent with high density of intraclasts. Drone images illustrating extensive scour in tidal channels: channel imaged (e) prior to Hurricane Irma and (f) after Hurricane Irma, when the entire channel was scoured to >3 m water depth. (g) Examples of lithified clasts transported into island interior, illustrating rare example of imbricated clasts. Scour pits near washover fans, including representative morphologies of (h) scour pits located immediately adjacent to a washover fan and (i) > 1-m deep scour in the lithified beach ridge to the south of washover fans.

arm of the hurricane; the primary record of Hurricane Irma conditions is therefore that gleaned from deposits formed during the second, northward flowing storm surge. Sediment properties of samples from adjacent areas are included in supporting information Table S3. Median grain sizes on the beach ridges, on the beach itself, and on the foreshore beneath the water are a few micrometers smaller than those in the washover fans and channel lobes (Tables 1 and S3). Sediment samples from the foreshore contained coarser skeletal grains, which were less abundant in sediment samples collected from the supratidal beach and beach ridges.

Table 1
Average Grain Characteristics of Sediment Samples From Washover Fans and Channel Lobes, as Well as Sediment Properties of Additional Samples Taken From Areas Adjacent to the Hurricane Deposits

	Washover fans (n = 77)	Channel lobes (n = 70)	Beach ridges (n = 3)	Beach (n = 2)	Foreshore (n = 2)
Average D_{50} (μm)	437	426	395	370	436
Average D_{10} (μm)	309	295	269	254	244
Average D_{90} (μm)	598	585	501	488	1,243
Average aspect ratio	1.26	1.29	1.28	1.33	1.35
Average roundness	0.74	0.75	0.72	0.68	0.65
Average sphericity	0.93	0.93	0.92	0.91	0.89

3.2. Channel Lobes

The channel lobe deposits are analogous to the formation of a washover fan, only with the sediment movement originating from the interior of the island rather than from the open platform. Their size range is between 200 and 410 m in length. Their position at the mouths of tidal channels suggest that these channels served as an outlet for the storm surge and accompanying sediment. We observed that the channel lobes were subjected to significant reworking over the ~2-year duration of our study by westward directed longshore currents and tidal currents, evidenced by their rapid westward migration (Figure 7) and changes in sediment properties, including an increase in median diameter of grains from 421 to 432 μm (supporting information Table S4).

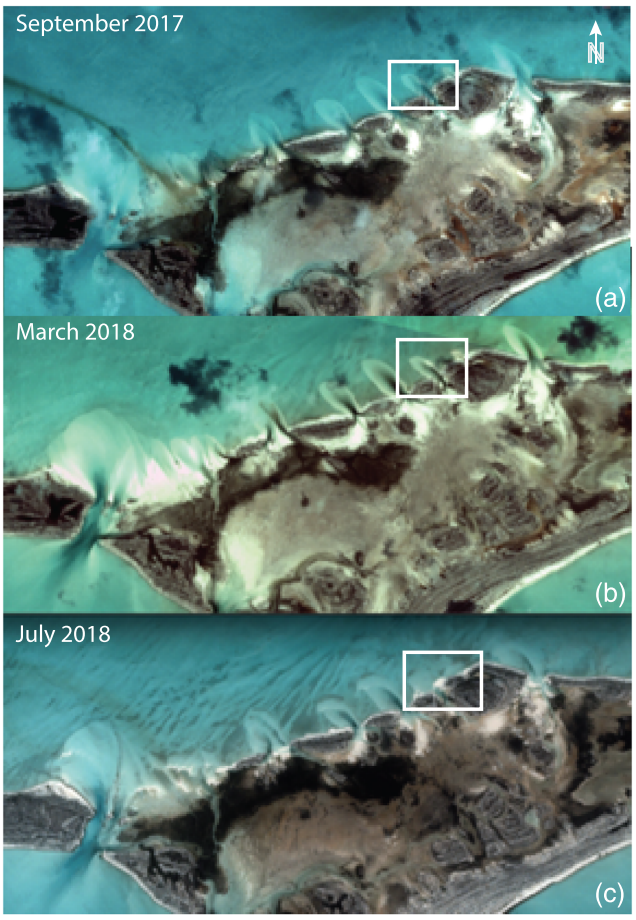

Figure 7. Channel lobe migration due to reworking by longshore currents. (top) September 2017, (middle) March 2018, and (bottom) July 2018. White boxes indicate the deposit that was eliminated by current reworking (images from Planet Team (2017). Planet Application Program Interface: In Space for Life on Earth. San Francisco, CA. https://api.planet.com).

Channel lobes were composed of very well sorted medium-sand-size ooids. The average of median grain diameters (D_{50}) across all samples from both March and June 2018 is 426 μm, with average sphericity 0.93, average aspect ratio 1.29, and average roundness 0.75. The average 10th percentile grain diameter (D_{10}) is 295 μm, and the average 90th percentile grain diameter (D_{90}) is 585 μm (Table 1).

There were no spatial trends in sediment size, shape, or sorting within or among the channel lobes from both the March 2018 and July 2018 sample sets, but there was evidence of significant reworking between March and July. Drone imagery showed a migration of about 10 m westward during this time, and the fan tips curved westward (Figure 7). This indicates reworking by westward longshore transport (Trower et al., 2018) that was not observable (or possible) in the location of the washover fans. Of the five channel lobes sampled, one of the eastern deposits was completely washed out by the longshore currents, so that it could no longer be sampled in July 2018. Differences in sorting and median grain size in the remaining four channel lobes show that the sediments were shifted over time, each lobe affected differently by tidal currents through each associated channel. The significance of the reworking over such a short time scale is that even the earliest (March 2018) set of samples was reflective of sediments that had already been altered from their original depositional state. The extent of channel lobe reworking also suggests that these deposits are ephemeral and may not be preserved in the rock record.

3.3. Washover Fans

Washover fans formed by Hurricane Irma on LAC are on the small end of the range of those that have been observed in previous studies, and they lack the sedimentary structures that are common to washover fans on continental coasts and barrier islands. They range from 23 to 118 m in length (parallel to the direction of sediment transport)

Figure 8. Representative trenches of washover fans from (top) March 2018 and (middle and bottom) June 2019. Laminations are due to compositional differences, mostly organics. Sorting and roundness are consistent throughout the trenches.

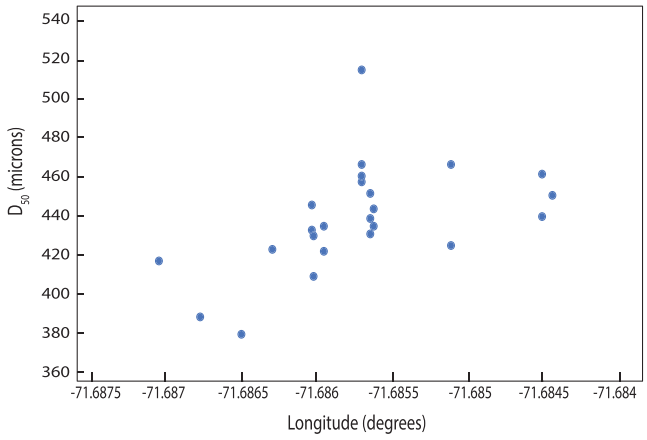

Figure 9. Median grain size increases moving from most eastern to most western sample sites.

and 16–49 m in width, while many previously studied washover fans are hundreds of meters long on average. Morton and Sallenger (2003) record fans ranging from 25 to 425 m in length. LAC washover fans range in thickness from 10 to 30 cm, whereas the thickness of typical washover fans ranges from 10 cm (Deery & Howard, 1977) to 1.5 m (Morton & Sallenger, 2003). Estimated sediment volumes in individual fans vary from 35 m^3 (smallest washover fan at a minimum depth of 10 cm) to 867 m^3 (largest washover fan at maximum depth of 30 cm) (supporting information Table S3).

Our observations indicate that unlike washover fans on continental coasts and barrier islands, the washover fans on LAC exhibit no notable variability grain size (i.e., grading) or sorting (Figure 8). While the deposits appeared massive, we cannot rule out the possibility that primary upper plane bed laminations in the deposits were obscured by the uniformity of the sediment in size, shape, and composition. The maximum storm strength and the height of the storm surge on LAC were unique to the direct passage of a storm over a low-lying island on a carbonate platform and most likely played a significant role in the unique features (or lack thereof) of these sediment deposits.

The washover fans on LAC follow the morphological pattern of those in other localities: They are located directly landward from the beach ridges and create a scalloped pattern along the edge of the island (Bourrouilh-Le, 1998). This pattern of deposition is similar to poststorm deposits on barrier islands, and LAC fans are consistent with the perched fan type described by Morton and Sallenger (2003). Perched fans sit atop the subaerial island surface landward of the beach ridges, as a result of a storm surge overtopping the topography. The washover fans occur in an area of the island where topography is relatively uniform along the beach and there are not many mangroves to interrupt flow (Supplementary Figure S8). The channel lobes on the northern shore have likely been subjected to more flow funneling through preexisting tidal channels.

The washover fans were less affected by poststorm event reworking, as they are perched on the inland edge of the southern side of the island and subjected only to shallow tidal flow in the interior lagoon. However, we observed that washover fan edges were encroached by microbial mats and one washover fan was transected due to a channel formed between the nearest scour pit and the main lagoon.

The washover fans are composed of very well sorted medium-sand-size oolitic sand (Table 1) with rare skeletal fragments and small microbial mat intraclasts. Median grain size increases from east to west over the washover fan area (Figure 9), but there are no spatial trends in sorting or grain shape (supporting information Table S6). There are no trends in grain size or sorting within individual fans. All of the washover fans are massively bedded, with good sorting and grain size consistent both across and along the length of each washover fan. The average median grain diameter (D_{50}) of all washover fan samples is 437 μm, while average sphericity is 0.93, average aspect ratio 1.26, and average roundness 0.74 (Table 1). The average 10th percentile grain diameter (D_{10}) is 309 μm, and the average 90th percentile (D_{90}) is 598 μm (Table 1). The surfaces of sand grains composing the fans are pinkish, as is the sand along the beach ridges,

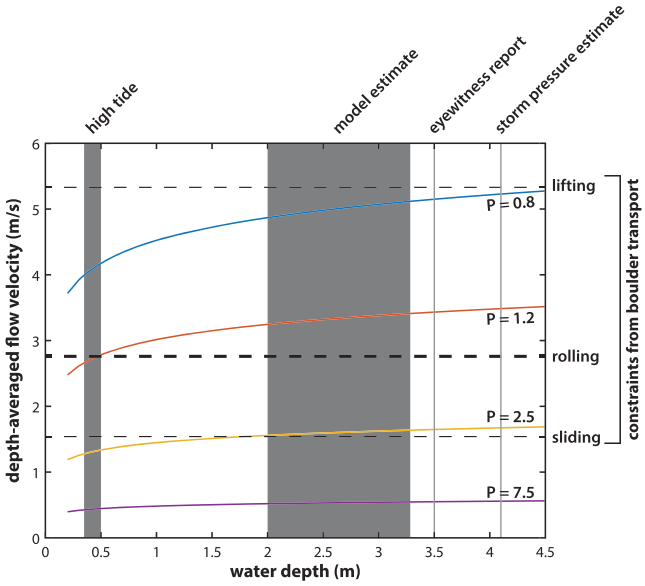

Figure 10. Flow velocities required to transport the sand composing the washover fans (colored lines) and the small boulders (dashed lines), at a wide range of storm surge depths, with constraints on depth shown with vertical lines. Observation of imbrication suggests that boulders were transported via rolling (bold dashed line). $P = 1.2$ corresponds to transport in suspension. See text for calculations and sediment descriptions.

while channel lobe sand is the more typical pearly hue of oolitic carbonate sediment. The average D_{50} of washover fan sediments is 11 μm larger than that of the channel lobe deposits (Table 1).

Scanning electron microscope (SEM) analysis showed that the pinkish coloration of the washover fan ooids was due to a biofilm produced by common microbial filaments (supporting information Figure S7) rather than a compositional difference that might have been indicative of sediment provenance.

3.4. Erosional Features

Erosional features include scour pits and lag deposits consisting of clasts of lithified Holocene sediment with intermediate axes ranging from 10 to 51 cm and composed of ooid grainstone and cobble-sized microbial mat intraclasts. The lag deposits occur in different locations, which is most likely due to different material densities. Measurements of the scour pits ($n = 9$) showed a length range of 2.3–16.3 m (average 7.3 m), a width range of 2.2–6 m (average 3.4 m), and a depth range of 0.2–1.2 m (average 0.54 m), showing considerable variability (supporting information Table S6). Calculated volumes have a range of 0.5–37.2 m^3 with an average displaced sediment volume of (9.5 m^3).

Flow velocity constraints using boulder dimension measurements yielded a range of 1.54–5.33 m/s, depending on the mode of transport (sliding, rolling, or lifting) (Figure 10). Our observation of imbrication (Figure 6g) requires transport via rolling (e.g., Master, 2013), implying a depth-averaged flow velocity of ≥2.8 m/s. Additional calculations following Terry et al. (2013) constrain the minimum velocity required to displace clasts of the size found on LAC to 2.6 m/s and the minimum storm surge height required to 0.9 m, both within our calculated ranges and consistent with boulder transport via rolling.

4. Discussion

4.1. Reconstructing Hurricane Flow Velocities

The flow velocities required to transport cobbles and small boulders into the interior of the island were beyond those that would be required to transport all of the sand grain sizes that compose the washover fans and channel lobes in suspension (Figure 10). This precludes net deposition during peak hurricane intensity. This interpretation applies across the range of constraints on depth of the storm surge, from the lower bound of high tide (~0.5 m) to the upper bound of the modeled storm surge (~3.23 m).

The channel lobes on the northern side of the island also support the interpretation of a high level of sediment bypass; their presence shows that enough sand was transported across the island during the northward storm surge to create large deposits on the northern side when flow velocities ebbed. Deep scours in the tidal channels associated with the lobe deposits also indicate high-energy flow. We interpret that the washover fans are composed of the sediment that was deposited once the storm energy began to wane and this bypass ceased. The slight decrease in grain size between the washover fans and channel lobes implies that smaller grains composing the channel lobes were deposited after the larger-grained washover fans and at a slightly lower flow velocity during the ebb of the storm surge. Given that during most of the storm event the flow velocities were too high for deposition, the deposits likely formed over a short time interval as the storm surge ebbed, potentially accounting for their small scale. Most of the previous studies on washover fans have focused on barrier islands that were not submerged at depth during the storms that affected them (Schwartz, 1982), but those that address inundation of islands during major storm events show that high volumes of sediment are carried landward across islands and then out to sea rather than deposited; inundation of barrier islands and atolls has produced low levels of sedimentation or no sedimentation, supporting our interpretation of sediment bypass on LAC (Lindemer et al., 2010; Sallenger, 2000; Sherwood et al., 2014). On carbonate platforms, there is sometimes no trace of deposition due to major storms at all (Boss &

Neumann, 1993; Reeder & Rankey, 2009). This suggests that the small, massively bedded deposits on LAC are likely the result of higher flow velocities and storm surge levels that submerged the area where the storm made landfall.

4.2. What Makes LAC Unique?

In environments with similar sediment sizes and types to the Caicos platform, storm deposits tend to be composed of well-sorted sand (see the Major et al., 1996, study of a Bahamian ooid shoal), which is consistent with the washover fans and channel lobes we observed. However, the sediment deposits on LAC associated with Hurricane Irma differ in several ways from most other examples of hurricane deposits. Both types of sediment bodies are formed as a result of the waning flow velocity following the passage of the storm surge, which allowed grains to be deposited from suspension. The massive bedding of the LAC washover fan deposits could be due to a number of factors that differentiate these deposits from those that have been addressed in previous studies. The allowance is often made for some variability among hurricane deposits, dependent on flow depth and topography (Morton & Sallenger, 2003), and there are some accounts of washover deposits that do not show internal structures (Sedgwick & Davis Jr., 2003). Washover fans lacking internal structures are rare and often occur adjacent to washover fans with graded bedding. Grading is commonly caused by a gradual decrease or increase in flow velocities over the course of a surge event, while on LAC the deposition of sand may have been more rapid. The beach ridges would have cut off flow as soon as the storm surge decreased sufficiently to no longer overtop the beach ridge topography, that is, after ~3 hr (supporting information Figure S4), causing all of the sediment in transport at that time to deposit at once. Massive bedding can occur when the time of deposition is not sufficient for internal structures to form (Leatherman & Williams, 1977, 1983). Many of the sedimentation patterns in other examples of washover fans are caused by repeated overwash events in a nonsubmerged setting (Schwartz, 1982), while on LAC much of the island was submerged throughout the storm. A northward directed flow over the duration of the peak storm surge would have resulted in >1.25-m-higher storm surge water levels on the south side of LAC than on the north side (supporting information Figure S4).

Sediments across LAC are relatively uniform (see Table 1), providing limited ranges of sediment size and sorting to source the deposits. The platform sediments adjacent to LAC are less well sorted than those of the washover fan deposits, with a higher degree of skeletal clasts, evidenced by higher aspect ratio and lower mean roundness and sphericity. Washover fan sediment is slightly coarser than that of the beach and beach ridge areas, with a higher proportion of ooids suggested by the higher mean roundness and sphericity relative to samples from foreshore sediments (Table 1). Washover fan sediment is probably sourced from a variety of environments, given that the leading arm of the storm had already scoured the area and the trailing arm of the storm deposited what was already in transport in the storm surge. It may also be difficult to detect primary sedimentary structures when sediment sources are so uniform; sediments that have good preexisting sorting and high roundness produce deposits with consistent sedimentary properties (Nichol & Kench, 2008). Therefore, the nature of grainy sediment on the Caicos platform may have obscured primary upper plane bed laminations, producing deposits that appear massive; these processes could also apply to strata deposited in ancient grainy carbonate platform settings.

Features such as mangroves and beach ridges may redirect or slow flow and play a more significant role in determining the locations and extent of hurricane deposits in other geological settings (Bourrouilh-Le, 1998; Suter et al., 1982; Wang & Horowitz, 2007), probably due to the more significant mangrove growth and ridge topography in continental coastal settings. LAC has scattered mangrove growth, but denser mangroves are primarily located on the northern side of the island, downcurrent from the washover fans. The beach ridges adjacent to the washover fans are topographically low, with a maximum elevation of 1.8 m that is consistent along the shore where the fans are situated (supporting information Figure S8). These beach ridges are covered with sea oats and patchy bushes of manchineel and sea grape tree. Field observations indicate these may have acted at a very small scale as flow barriers and at the same time have funneled flow in less vegetated corridors. The channel lobes may have been subjected to more spatially confined flow due to flow concentration in preexisting tidal channels, minimizing the effect of denser red and black mangrove growth between channels.

Bioturbation also plays a significant role in reworking hurricane deposits in most instances (Deery & Howard, 1977), while on LAC there was a lack of burrowing and other reworking of the sediments; the

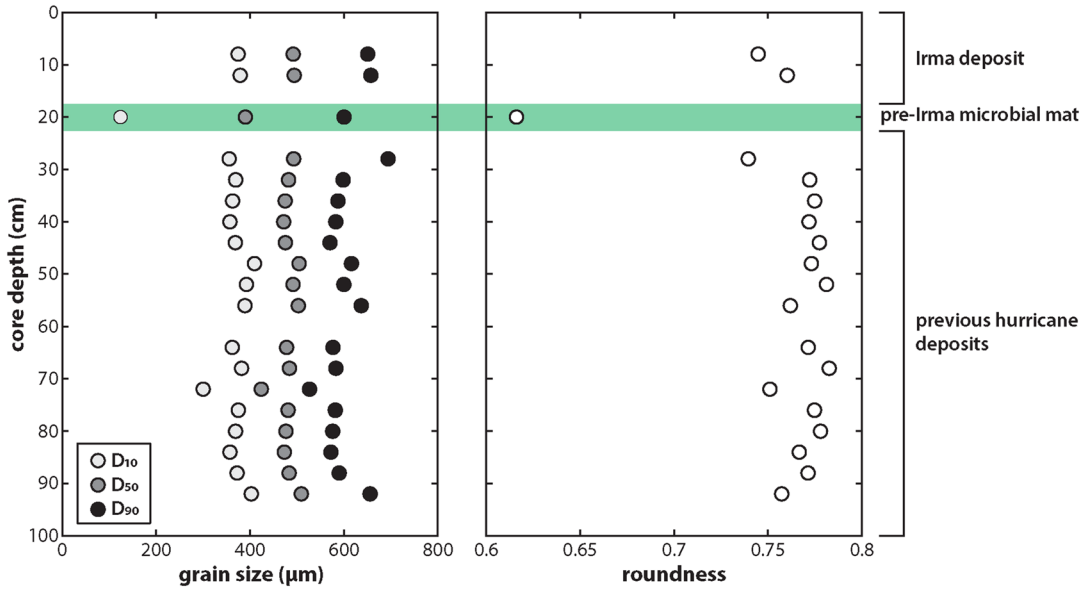

Figure 11. Grain size and roundness data of a sediment core from a washover fan on LAC. A series of hurricane-related deposits beneath the current washover fan show similar sediment properties.

only biological influence observed was the gradual regrowth of surface microbial mats over the 2 years following the hurricane (supporting information Figure S9), which did not substantially alter any sedimentary structures within the fans. Nearshore bathymetry and the depth of an interior lagoon can also affect the force and depth of the storm surges that form these deposits (Harris & Ellis, 2008; Pierce, 1970). The bathymetry off the coast of LAC is characteristic of a shallow-marine carbonate shelf, with no near-shore reefs to redirect the storm surge or break the strength of the surge. The flow depth and velocity during Hurricane Irma were significant, submerging the island nearly completely and allowing for extensive sediment transport (Harris & Ellis, 2008).

4.3. Identifying LAC-Type Hurricane Deposits in the Rock Record

The hurricane deposits described in this study differ from those described in previous studies in both the geological setting and storm conditions. These deposits are associated with a massive open ocean storm event on a low-topography carbonate platform, different from more topographically complex continental coasts experiencing oblique storm trajectories. The Caicos platform is often used as an analogue for ancient carbonate depositional environments (Dravis & Wanless, 2017); our observations suggest that even large hurricanes may commonly only produce small, ungraded washover fans on carbonate platforms. The similarity and uniformity of sediment characteristics of the cored interval underlying the Irma washover fans indicates that Irma deposits are representative of typical hurricane deposition on LAC (Figure 11). This shows that it is possible to identify a repeated, distinct sequence indicative of hurricane events in the rock record of a carbonate platform. Similar features have also been observed in the Turks and Caicos Islands after Hurricanes Hannah and Ike, which further suggests that the depositional effects of hurricanes on LAC are repeatable (Bachtel et al., 2011). Most of the island was characterized by neither net deposition nor net erosion during the hurricane, leaving no overall stratigraphic signal beyond these localized deposits. The uniformity of the size and shape of sediment on a grainy carbonate platform could obscure primary sedimentary structures (e.g., plane lamination or grading), resulting in deposits that appear massive. This indicates that small, massively bedded washover fans in the rock record may counterintuitively indicate large storm events, as they are examples of the ebb of a major storm and not its peak energy, which causes sediment bypass rather than deposition to occur (Boss & Neumann, 1993; Lindemer et al., 2010; Reeder & Rankey, 2009; Sallenger, 2000; Sherwood et al., 2014). Given the difficulty of identifying massive beds that are neither vertically nor laterally extensive, this type of deposit may be largely unrecognized in the rock record. The nature of the hurricane deposits and erosive features on the island is ephemeral; the washover deposits are small in size and difficult to identify, while the channel lobes are subject to dispersal by currents and the scour pits are

likely to be infilled during high tides. The position of washover fans "perched" on the subaerial island surface creates the potential for preservation where other deposits subject to reworking by currents, such as the channel lobes, are unlikely to be preserved (Hudock et al., 2014). A combination of erosional features such as channel and pit scour and lag deposits adjacent to small massive sand bodies may be used to confirm the presence of a major storm event.

5. Conclusions

The depositional signature of hurricanes in a carbonate platform setting is distinct from that on coastlines adjacent to continental shelves. By examining the sedimentary properties and dimensions of these types of deposits, as well as associated erosional features, we have been able to delineate a new model for a distinct type of hurricane deposit. Key characteristics of hurricane deposition on a carbonate platform are relatively small size (tens of meters in length and tens of centimeters in depth, well-sorted sediment, and massive bedding), and large storms are likely to produce small-scale or no erosional and depositional features. Large storms are also associated with high storm surges and high flow velocities, which can be constrained by modeling, observation of erosional features, and empirical calculation. Using the description we have provided, it may be possible to identify previously unrecognized storm events in the carbonate rock record, and to use this framework to better understand the modes of sediment transport associated with modern and future hurricane deposits on carbonate platforms.

Data Availability Statement

The raw data associated with Camsizer, tidal current velocity, and tide gauge measurements are available at https://doi.org/10.17605/OSF.IO/UNTGP.

Acknowledgments
This work was supported by the Agouron Institute Grant SGIA-277.19.1UCB, NASA Exobiology Grant 80NSSC18K0278, and the CU Boulder Department of Geological Sciences. The authors acknowledge logistical support from Paul Mahoney and James Seymour and field assistance from Maya Gomes, Alistair Hayden, Usha Lingappa, Taleen Mahseredjian, and Theodore Present. Pim Maydhisudhiwongs ran Camsizer analyses of WF-J18 core samples. This project was carried out under Scientific Research Permit 19-06-01-20 from the Department of Environment and Coastal Resources of the Turks and Caicos Islands. S. J. T. thanks David Budd and Katherine Lininger for helpful feedback. We thank Evan Goldstein, Katherine Anarde, and two anonymous reviewers for their constructive reviews.

References

Bachtel, S., Kerans, C., & Bachtel, C. I. (2011). The sedimentary influences of Hurricanes Hannah and Ike (September 2008) on the Caicos platform, B.W.I.: Do high-energy storms impact sedimentation on carbonate platforms? AAPG abstract.

Bergantino, R. N. (1971). Submarine regional geomorphology of the Gulf of Mexico. *GSA Bulletin*, *82*(3), 741–752. https://doi.org/10.1130/0016-7606(1971)82[741:SRGOTG]2.0.CO;2

Booij, N., Lis, R. C., & Holthuijsen, L. H. (1999). A third-generation wave model for coastal regions 1. Model description and validation. *Journal of Geophysical Research*, *104*(C4), 7649–7666. https://doi.org/10.1029/98JC02622

Boss, S. K., & Neumann, A. C. (1993). Impacts of Hurricane Andrew on carbonate platform environments, northern Great Bahama Bank. *Geology*, *21*(10), 897–900. https://doi.org/10.1130/0091-7613(1993)021%3C0897:IOHAOC%3E2.3.CO;2

Bourrouilh-Le, J. (1998). The role of high-energy events (hurricanes and/or tsunamis) in the sedimentation, diagenesis and karst initiation of tropical shallow water carbonate platforms and atolls. *Sedimentary Geology*, *118*(1–4), 3–36. https://doi.org/10.1016/S0037-0738(98)00003-7

Bryant, W. R., Antoine, J., Ewing, M., & Jones, B. (1968). Structure of Mexican continental shelf and slope, Gulf of Mexico. *AAPG Bulletin*, *52*(7), 1204–1228.

Cangialosi, J. P., Latto, A. S., & Berg, R. (2017). National Hurricane Center tropical cyclone report, NOAA.

Deery, J. R., & Howard, J. D. (1977). Origin and character of washover fans on the Georgia Coast, U.S.A. *transactions of GCAGS*, *27*, 259–271.

Dietrich, J. C., Zijlema, M., Westerink, J. J., Holthuijsen, L. H., Dawson, C., Luettich, R. A., et al. (2011). Modeling hurricane waves and storm surge using integrally-coupled, scalable computations. *Coastal Engineering*, *58*(1), 45–65. https://doi.org/10.1016/j.coastaleng.2010.08.001

Dietrich, W. E. (1982). Settling velocity of natural particles. *Water Resources Research*, *18*(6), 1615–1626.

Dravis, J. J. & Wanless, H. R. (2008). Caicos platform models of quaternary carbonate deposition controlled by stronger easterly trade winds —Application to petroleum exploration, in Morgan, W. A., and P. M. Harris, eds., Developing models and analogs for isolated carbonate platforms—Holocene and Pleistocene carbonates of Caicos platform, British West Indies, SEPM, Core Workshop Notes, 22, 21–27.

Dravis, J. J., & Wanless, H. R. (2017). Impact of strong easterly trade winds on carbonate petroleum exploration—Relationships developed from Caicos platform, southeastern Bahamas. *Marine and Petroleum Geology*, *85*(1), 272–300. https://doi.org/10.1016/j.marpetgeo.2017.04.010

Egbert, G. D., & Erofeeva, S. Y. (2002). Efficient inverse modeling of barotropic ocean tides. *Journal of Atmospheric and Oceanic Technology*, *19*(2), 183–204. https://doi.org/10.1175/1520-0426(2002)019%3C0183:EIMOBO%3E2.0.CO;2

Garzon, J. L., Ferreira, C. M., & Padilla-Hernandez, R. (2018). Evaluation of weather forecast systems for storm surge modeling in the Chesapeake Bay. *Ocean Dynamics*, *68*(1), 91–107. https://doi.org/10.1007/s10236-017-1120-x

Goff, J. A., Swartz, J. M., Gulick, S. P. S., Dawson, C. N., & de Alegria-Arzaburu, A. R. (2019). An outflow event on the left side of Hurricane Harvey: Erosion of barrier sand and seaward transport through Aransas Pass, Texas. *Geomorphology*, *334*, 44–57. https://doi.org/10.1016/j.geomorph.2019.02.038

Harris, P. M. & Ellis, J. (2008). Satellite imagery and visualization of the Caicos platform, in Developing models and analogs for isolated carbonate platforms—Holocene and Pleistocene carbonates of Caicos platform, British West Indies, SEPM, Core Workshop, 22, 29–46.

Hudock, J. W., Flaig, P. P., & Wood, L. J. (2014). Washover fans: A modern geomorphologic analysis and proposed classification scheme to improve reservoir models. *Journal of Sedimentary Research*, *84*(10), 854–865. https://doi.org/10.2110/jsr.2014.64

Kerans, C., Zahm, C., Bachtel, S. L., Hearty, P., & Cheng, H. (2019). Anatomy of a late Quaternary carbonate island: Constraints on timing and magnitude of sea-level fluctuations, West Caicos, Turks and Caicos Islands, BWI. *Quaternary Science*, *205*, 193–223. https://doi.org/10.1016/j.quascirev.2018.12.010

Lazarus, E. D. (2016). Scaling laws for coastal overwash morphology. *Geophysical Research Letters*, *43*, 12,113–12,119. https://doi.org/10.1002/2016GL071213

Leatherman, S. P., & Williams, A. T. (1977). Lateral textural grading in overwash sediments. *Earth Surface Processes and Landforms*, *2*(4), 333–341. https://doi.org/10.1002/esp.3290020406

Leatherman, S. P., & Williams, A. T. (1983). Vertical sedimentation units in a barrier island washover fan. *Earth Surface Processes and Landforms*, *8*(2), 141–150. https://doi.org/10.1002/esp.3290080205

Li, H., Lin, L., & Burks-Copes, K. A. (2013). Modeling of coastal inundation, storm surge, and relative sea-level rise at Naval Station Norfolk, Norfolk, Virginia, U.S.A. *Journal of Coastal Research*, *286*, 18–30. https://doi.org/10.2112/JCOASTRES-D-12-00056.1

Lindemer, C. A., Plant, N. G., Puleo, J. A., Thompson, D. M., & Wamsley, T. V. (2010). Numerical simulation of a low-lying barrier island's morphological response to Hurricane Katrina. *Coastal Engineering Journal*, *57*(11–12), 985–995. https://doi.org/10.1016/j.coastaleng.2010.06.004

Luettich, R. A., Westerink, J. J., & Scheffner, N. W. (1992). ADCIRC: An advanced three-dimensional circulation model for shelves, coasts, and estuaries. Report 1. Theory and methodology of ADCIRC-2DDI and ADCIRC-3DL.

Major, R. P., Bebout, D. G., & Harris, P. M. (1996). Recent evolution of a Bahamian ooid shoal: Effects of Hurricane Andrew. *Geological Society of America Bulletin*, *108*(2), 168–180. https://doi.org/10.1130/0016-7606(1996)108%3C0168:REOABO%3E2.3.CO;2

Master, S. (2013). A note on imbricated granite boulders on NW Penang Island, Malaysia: Tsunami or storm origin? *NTHR*, *35*, 225–241.

Mattheus, C. R., & Fowler, J. K. (2015). Paleotempestite distribution across an isolated carbonate platform, San Salvador Island, Bahamas. *Journal of Coastal Research*, *31*(4), 842–858.

Morton, R. A., & Sallenger, A. H. Jr. (2003). Morphological impacts of extreme storms on sandy beaches and barriers. *Journal of Coastal Research*, *19*(3), 560–573.

Nandasena, N. A. K., Paris, R., & Tanaka, N. (2011). Reassessment of hydrodynamic equations: Minimum flow velocity to initiate boulder transport by high energy events (storms, tsunamis). *Marine Geology*, *281*, 70–84.

Nichol, S. L., & Kench, P. S. (2008). Sedimentology and preservation potential of carbonate sand sheets deposited by the December 2004 Indian Ocean tsunami: South Baa Atoll, Maldives. *Sedimentology*, *55*(5), 1173–1187. https://doi.org/10.1111/j.1365-3091.2007.00941.x

Nott, J. (2003). Waves, coastal boulder deposits and the importance of the pre-transport setting. *Earth Planetary Science Letter*, *210*(1-2), 269–276. https://doi.org/10.1016/S0012-821X(03)00104-3

Orzechowski, E., Strauss, J., Knoll, A, Fischer, W., Cantine, M., Metcalfe, K., et al. (2016). Age and construction of Little Ambergris Cay bedrock rim, southeastern Caicos Platform, British West Indies, AGU Fall Meeting Proceedings, Abstract.

Pierce, J. W. (1970). Tidal inlets and washover fans. *Journal of Geology*, *78*(2), 230–234. https://doi.org/10.1086/627504

Planet Team (2017). *Planet application program interface: In space for life on Earth*. San Francisco, CA. https://api.planet.com

Pomar, L. (2001). Types of carbonate platforms: A genetic approach. *Basin Research*, *13*(3), 313–334. https://doi.org/10.1046/j.0950-091x.2001.00152.x

Read, J. F. (1982). Carbonate platforms of passive (extensional) continental margins: Types, characteristics, and evolution. *Tectonophysics*, *81*(3–4), 195–212. https://doi.org/10.1016/0040-1951(82)90129-9

Reeder, S. L., & Rankey, E. C. (2009). A tale of two storms: An integrated field, remote sensing and modeling study examining the impact of Hurricanes Frances and Jeanne on carbonate systems, in Perspectives in carbonate geology: A tribute to the career of Robert Nathan Ginsburg. *International Association of Sedimentologists. Special Publication*, 75–90.

Roberts, K. J., Pringle, W. J., & Westerink, J. J. (2019). OceanMesh2D 1.0: MATLAB-based software for two-dimensional unstructured mesh generation in coastal ocean modeling. *Geoscientific Model Development*, *12*(5), 1847–1868. https://doi.org/10.5194/gmd-12-1847-2019

Sahoo, B., Jose, F., & Bhaskaran, P. K. (2019). Hydrodynamic response of Bahamas archipelago to storm surge and hurricane generated waves—A case study for Hurricane Joaquin. *Ocean Engineering*, *184*, 227–238. https://doi.org/10.1016/j.oceaneng.2019.05.026

Sallenger, A. H. Jr. (2000). Storm impact scale for Barrier Islands. *Journal of Coastal Research*, *16*(3), 890–895.

Schwartz, R. K. (1982). Bedform and stratification characteristics of some modern small-scale washover sand bodies. *Sedimentology*, *29*(6), 835–849. https://doi.org/10.1111/j.1365-3091.1982.tb00087.x

Sedgwick, P. E., & Davis, R. A. Jr. (2003). Stratigraphy of washover deposits in Florida: Implications for recognition in the stratigraphic record. *Marine Geology*, *200*(1–4), 31–48. https://doi.org/10.1016/S0025-3227(03)00163-4

Shaw, J., You, Y., Mohrig, D., & Kocurek, G. (2015). Tracking hurricane-generated storm surge with washover fan stratigraphy. *Geology*, *43*(2), 127–130. https://doi.org/10.1130/G36460.1

Sherwood, C. R., Long, J. W., Dickhudt, P. J., Dalyander, P. S., Thompson, D. M., & Plant, N. G. (2014). Inundation of a barrier island (Chandeleur Islands, Louisiana, USA) during a hurricane: Observed water-level gradients and modeled seaward sand transport. *Journal of Geophysical Research: Earth Surface*, *119*, 1498–1515. https://doi.org/10.1002/2013JF003069

Soria, J. L. A., Switzer, A. D., Pilarczyk, J. E., Tang, H., Weiss, R., Siringan, F., et al. (2018). Surf beat-induced over wash during Typhoon Haiyan deposited two distinct sediment assemblages on the carbonate coast of Hernani, Samar, central Philippines. *Marine Geology*, *396*, 215–230. https://doi.org/10.1016/j.margeo.2017.08.016

Spiske, M., & Jaffe, B. E. (2009). Sedimentology and hydrodynamic implications of a coarse-grained hurricane sequence in a carbonate reef setting. *Geology*, *37*(9), 839–842. https://doi.org/10.1130/G30173A.1

Stein, N., Quinn, D. P., Grotzinger, J. P., Fischer, W. W., Knoll, A. H., Cantine, M., et al. (2016). UAV, DGPS, and laser transit mapping of microbial mat ecosystems on Little Ambergris Cay, B.W.I., SAO/NASA, Abstract.

Suter, J. R., Nummedal, D., Maynard, A. K., & Kemp, P. (1982). A process-response model for hurricane washovers, Coast. Eng. J., 18th International Conference on Coastal Engineering.

Terry, J. P., Lau, A. Y. A., & Etienne, S. (2013). *Reef-platform coral boulders: Evidence for high energy marine inundation events on tropical coastlines*. Singapore: Springer Briefs in Earth Sciences. https://doi.org/10.1007/978-981-4451-33-8

Tozer, B., Sandwell, D. T., Smith, W. H. F., Olson, C., Beale, J. R., & Wessel, P. (2019). Global bathymetry and topography at 15 arc sec: SRTM15+.

Trower, E. J., Cantine, M. D., Gomes, M. L., Grotzinger, J. P., Knoll, A. H., Lamb, M. P., et al. (2018). Active ooid growth driven by sediment transport in a high-energy shoal, Little Ambergris Cay, Turks and Caicos Islands. *Journal of Sedimentary Research*, *88*(9), 1132–1151. https://doi.org/10.2110/jsr.2018.59

Wang, P., & Horwitz, M. H. (2007). Erosional and depositional characteristics of regional overwash deposits caused by multiple hurricanes. *Sedimentology*, *54*(3), 545–564. https://doi.org/10.1111/j.1365-3091.2006.00848.x

Wanless, H. R., Tyrell, K. M., Tedesco, L. P., & Dravis, J. J. (1988). Tidal-flat sedimentas, Caicos platform, British West Indies. *Journal of Sedimentary Research*, *58*(4), 724–738.

Wessel, P., & Smith, W. H. F. (1996). A global, self-consistent, hierarchical, high-resolution shoreline database. *Journal of Geophysical Research*, *101*, 8741–8743.

Wesselman, D., de Winter, R., Oost, A., Hoekstra, P., & van der Vegt, M. (2019). The effect of washover geometry on sediment transport during inundation events. *Geomorpholoy*, *327*, 28–47. https://doi.org/10.1016/j.geomorph.2018.10.014

Westerink, J. J., Luettich, R. A., Feyen, J. C., Atkinson, J. H., Dawson, C., Roberts, H. J., et al. (2008). A basin- to channel-scale unstructured grid hurricane storm surge model applied to southern Louisiana. *Monthly Weather Review*, *136*(3), 833–864. https://doi.org/10.1175/2007MWR1946.1

Williams, H. D., Burgess, P. R., Wright, V. P., Porta, G. D., & Granjeon, D. (2011). Investigating carbonate platform types: Multiple controls and a continuum of geometries. *Journal of Sedimentary Research*, *81*(1), 18–37.

Wilson, J. L. (1974). Characteristics of carbonate-platform margins. *AAPG Bulletin*, *58*(5), 810–824.

Wilson, K., Hassenruck-Gudipati, H. J., Mason, J., Schroeder, C. L., Smith, B., & Mohrig, D.C. (2018). Coastal impacts from far field storms—Evidence from Eleuthera, The Bahamas, AGU Fall Meeting 2018, Abstract.